NORWEGIAN JOURNAL OF GEOLOGY
https://dx.doi.org/10.17850/njg103-2-1

GEOLOGICAL SOCIETY OF NORWAY

Bivalve beds reveal rapid changes in ocean oxygenation in the Boreal Middle Triassic – a case study from Svalbard, Norway

Victoria S. Engelschiøn[1], Sofie Bernhardsen[2, 4], Fredrik Wesenlund[3, 5], Øyvind Hammer[1], Jørn H. Hurum[1] and Atle Mørk[2]

[1]*The Natural History Museum, University of Oslo, P.O. Box 1172 Blindern, NO–0318 Oslo, Norway*
[2]*The Norwegian University of Sciences and Technology, P.O. Box 8900, Torgarden, NO–7491 Trondheim, Norway*
[3]*The Arctic University of Norway, P.O. Box 6050 Langnes, N–9037 Tromsø, Norway*
[4]*Equinor, Margrethe Jørgensens vei 4, 9406 Harstad, Norway*
[5]*Applied petroleum technology AS, Sven Oftedals vei 6, 0950 Oslo, Norway*

E-mail corresponding author (Victoria S. Engelschiøn) v.s.engelschion@nhm.uio.no

Keywords:
- *Middle Triassic*
- *Svalbard*
- *Black shales*
- *Daonella*
- *Triassic bivalves*

Electronic supplement 1: Engelschiøn et al_data SI.xlsx

Received:
4. December 2022

Accepted:
6. March 2023

Published online:
17. March 2023

A fossil-rich interval in the organic-rich marine black mudstone of the Middle Triassic Botneheia Formation on eastern Svalbard was logged in high-resolution on an extremely well exposed section with emphasis on bivalve beds, taphonomic features, trace fossils and oxygenation proxies. The size distribution, fragmentation, articulation and orientation of three bivalve beds of the epifaunal flat clam *Daonella* were analysed. The logged section was studied for the recurrent occurrences of trace fossils and bivalve beds, and size distribution of framboidal pyrite. *Daonella* is most common in the shaly interval, while other taxa seem to outcompete *Daonella* in the siltier intervals. The comparison of fossil and sedimentological data with geochemical proxies for oxygenation revealed that the bivalve beds formed under dysoxic, conditions and due to low sedimentation rates and winnowing are not mass-mortality assemblages as previously suggested. The deposition on the sea floor was interrupted by anoxic intervals without benthic life. Recurrent beds containing the trace fossil *Thalassinoides*, however, show that oxygen levels fluctuated. The combination of water currents and oxygen fluctuations is a key to understanding why the black shales of the Botneheia Formation are so rich in benthic fossils.

Engelschiøn, V.S., Bernhardsen, S., Wesenlund, F., Hammer, Ø., Hurum, J.H. & Mørk, A. 2023: Bivalve beds reveal rapid changes in ocean oxygenation in the Boreal Middle Triassic – a case study from Svalbard, Norway. *Norwegian Journal of Geology 103*, 202306. https://dx.doi.org/10.17850/njg103-2-1

Introduction

The Middle Triassic Botneheia Formation in Svalbard (Fig. 1) consists of organic-rich black shales deposited under fluctuating oxic to anoxic conditions (Fig. 2–4) (Mørk & Bjorøy, 1984; Krajewski, 2008; Krajewski, 2013; Vigran et al., 2014; Wesenlund et al., 2021). The formation is characterised by an abundant benthic fauna with mass occurrences of *Daonella degeeri* (Böhm, 1912) preserved in bivalve beds (Fig. 3–5A). These have been interpreted as mass-mortality events caused by temporary euxinia (Krajewski, 2008). In this study, we aim to further understand the sedimentological environment of the Botneheia Formation. This has been considered a paradox in the Botneheia Fm., as the formation is characterised by high-organic richness indicating oxygen deficiency, combined with an abundant benthic fauna.

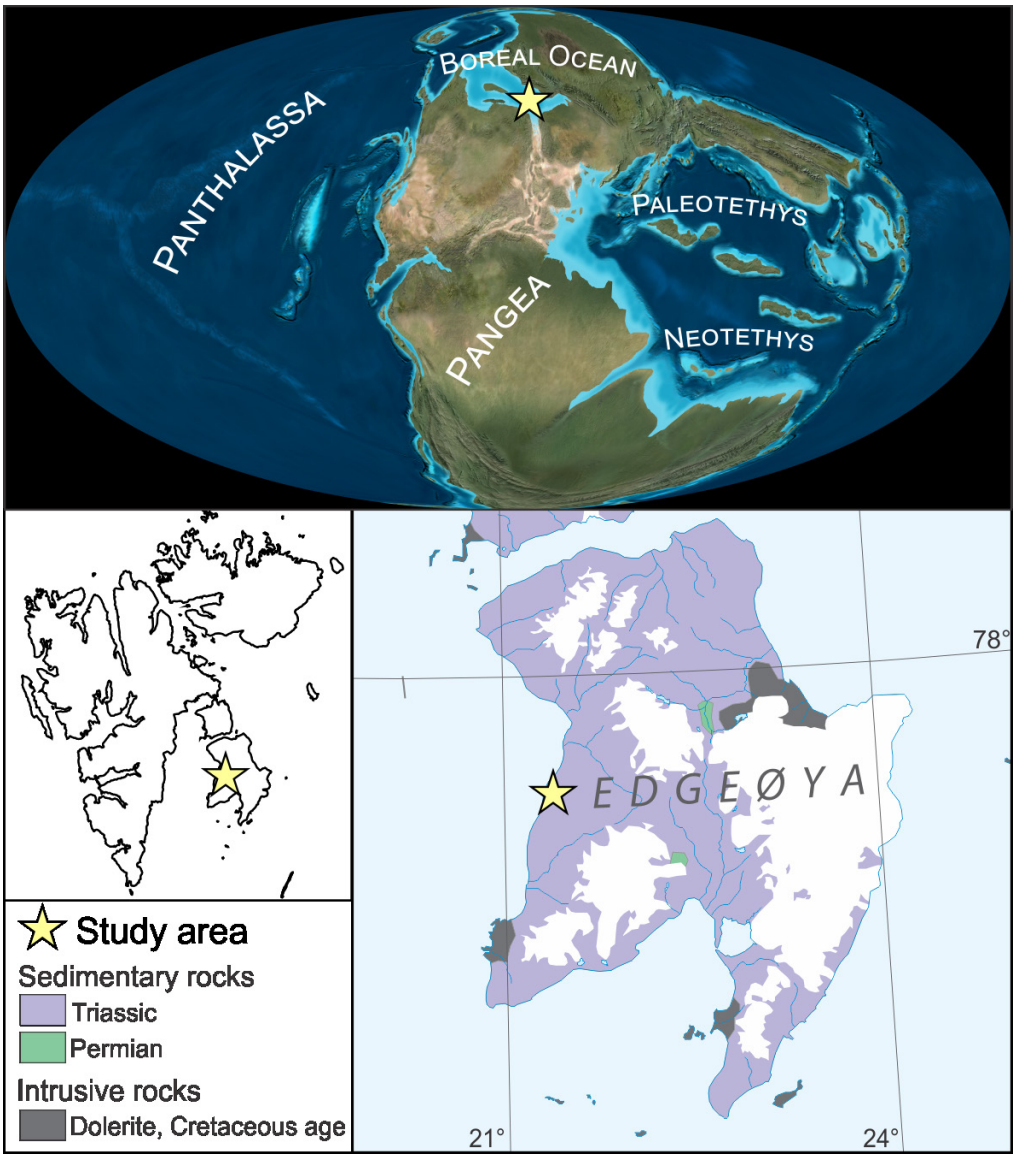

Figure 1. Palaeogeographical reconstruction of Pangea © 2013 Colorado Plateau Geosystems Inc, licence #110719. Study site marked by asterisk. The island of Edgeøya is part of the Arctic archipelago of Svalbard, and Triassic rocks crop out over the entire island. Geological map modified from Dallmann (2015).

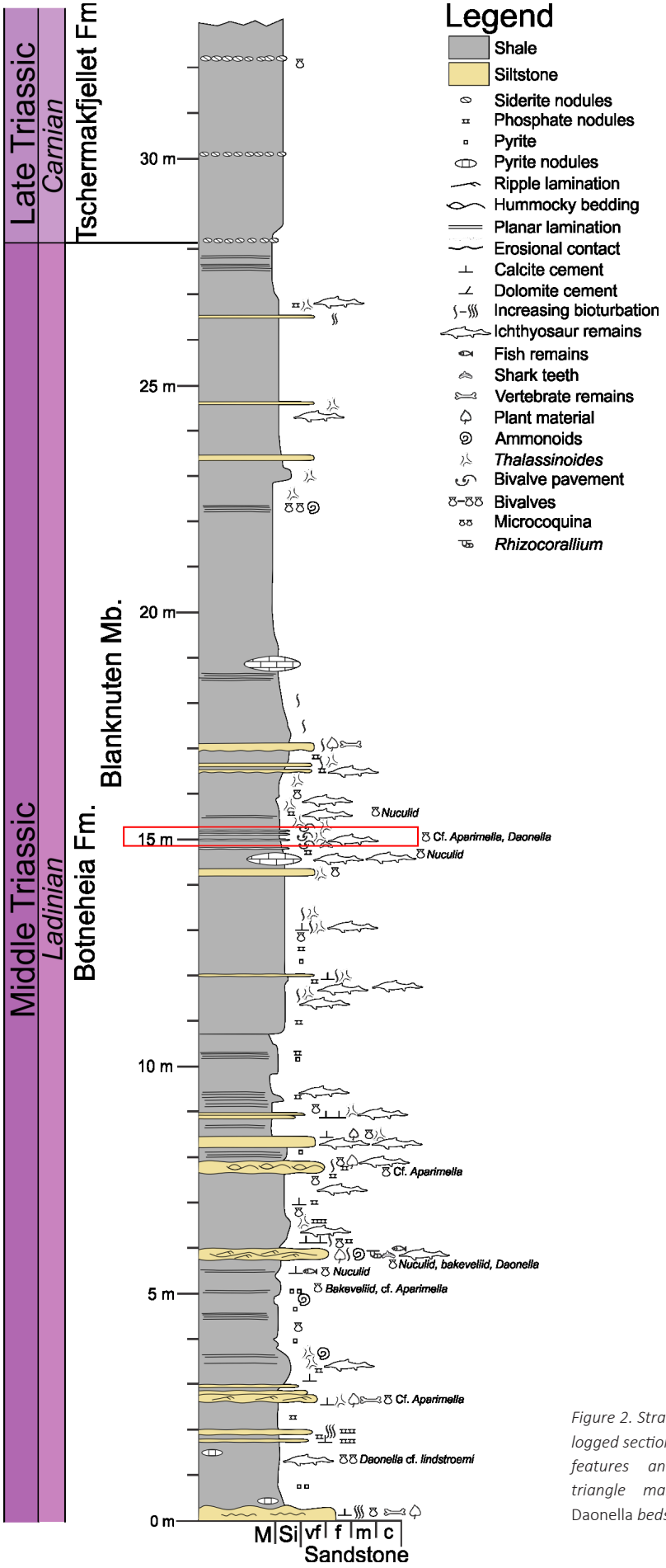

Figure 2. Stratigraphic column of the logged section with sedimentological features and fossil finds. Red triangle marks the position of Daonella *beds 1–3.*

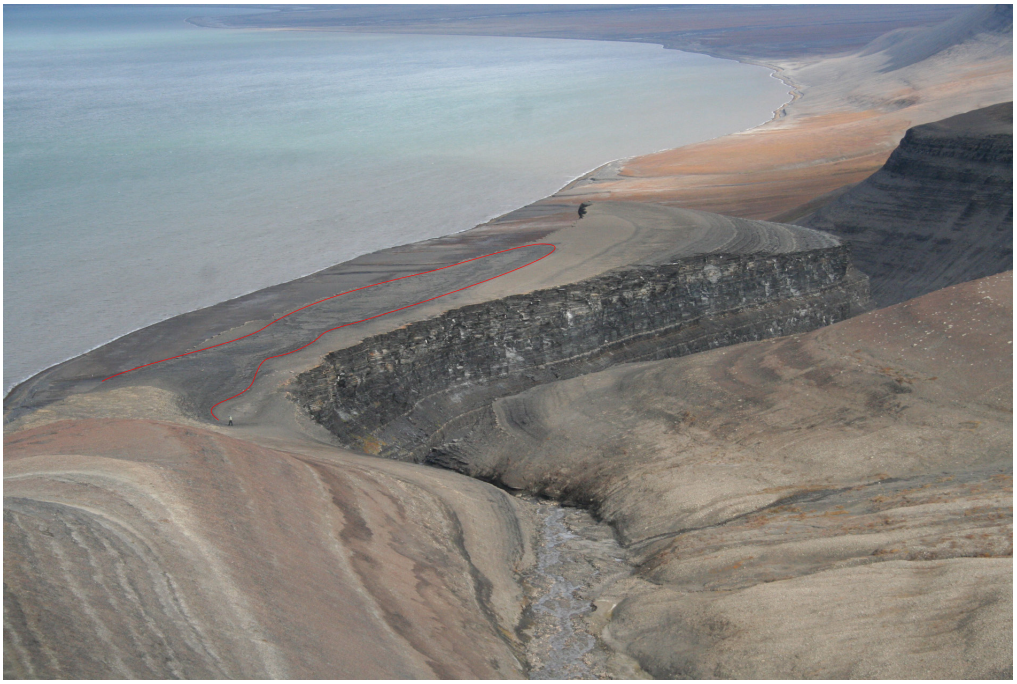

Figure 3. Photograph of the Muen plateau, the red outline marks the exposure of the Daonella beds 1–3. Photo by A.M.

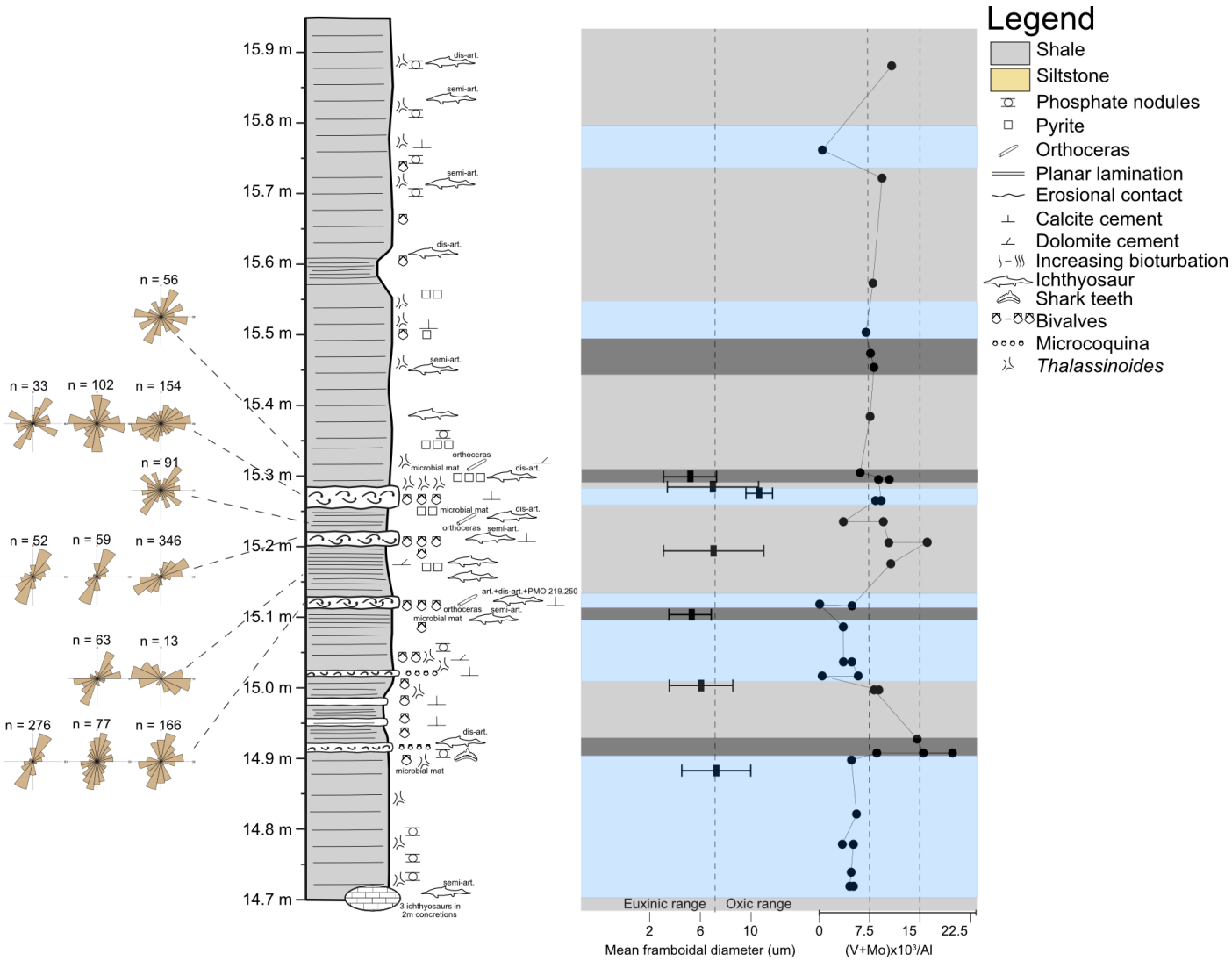

*Figure 4. Zoom-in on the stratigraphical column of the Muen plateau. Symbols mark body fossils, trace fossils, and microbial mats. The degree of articulation of ichthyosaurs is indicated. Colours denote oxygenation state. Blue = oxygenated, grey = dysoxic, dark grey = anoxic. Rose plots show degree of shell orientation in different beds. Plot of framboidal pyrite sizes, and the ((V + Mo) * 1000) / Al values. Abbreviations: art = articulated.*

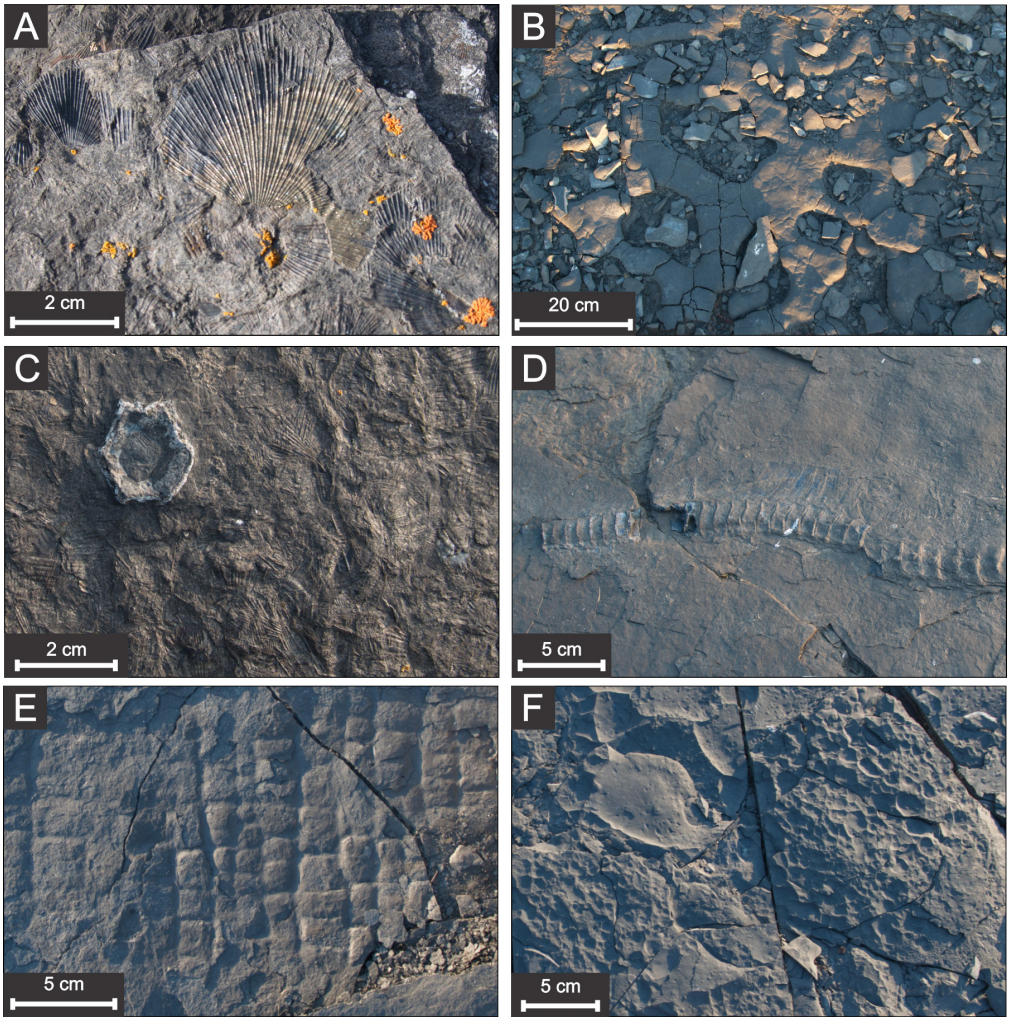

Figure 5. Fossil preservation on the Muen plateau. (A) The epifaunal flat clam Daonella degeeri, *partly covered by pyrite. (B) Phosphatised and connected burrows of the trace fossil* Thalassinoides. *(C) Disarticulated mixosaurid vertebra. Isolated bones were scattered across the bedding surfaces. (D) Partly articulated spine of mixosaurid, commonly found in the* Daonella *beds. (E) Algal mat («elephant skin»). (F) Algal mat («bubble texture»).*

Black shales and mudstones

The properties of black shales and mudstones are partly determined by the prevailing oxygen conditions during deposition (e.g., Savrda & Bottjer, 1989; MacQuaker & Gawthorpe, 1993; MacQuaker et al., 2010). Oxygen-deficient environments can provide excellent fossil preservation potential, and some of the most fossil-rich rocks in the world (Lagerstätten) are black shales. Temporal variations in oxygenation are caused by a variety of factors. These include changes in the depositional regime due to sea-level change, variable ocean currents, water mass stratification, large algal blooms (especially in upwelling zones), opening or closing of seaways, storms, and climatic variations. Rhoads & Morse (1971) described three oxygen-controlled biofacies: aerobic (O_2 > 1 ml/L), dysaerobic (O_2 = 0.1–1 ml/L) and azoic (O_2 < 0.1 ml/L, replaced by the term anaerobic by Byers (1977)). Another biofacies is poikiloaerobic (where short-term fluctuations are providing the necessary O_2 for opportunists) defined by Oschmann (1991). Anoxic and anaerobic differ in that the former refers to dissolved oxygen levels, while the latter refers to modes of life or biofacies (Allison et al., 1995). Euxinic is an additional term used to describe anoxic water masses with hydrogen sulphide (Allison et al., 1995; Lyons & Severmann, 2006). Ocean anoxia is thought to be one of the driving killing mechanisms in the Early Triassic, and has

been shown to be an overarching control on recovery patterns after the end-Permian extinction (EPME) (e.g., Wignall & Twitchett, 1996; Hotinski et al., 2001; Bottjer et al., 2008; Clapham & Payne, 2011; Pietsch & Bottjer, 2014; Song et al., 2014; Bond & Grasby, 2017; Benton, 2018; Zhang et al., 2018). Marine redox conditions in the Tethyan Ocean are thought to have reached the well-oxygenated pre-EPME levels only in the early Middle Triassic (Lau et al., 2016). Less is known about Boreal oxygenation in the Middle Triassic, but Early Triassic studies have shown that oxygen depletion was more severe in Boreal regions than in the Tethyan realm (Bond & Wignall, 2010; Dustira et al., 2013; Grasby et al., 2016).

Bivalve beds

Bivalve shell accumulations result from a combination of different palaeoenvironmental processes (see extensive literature list in Posenato et al., 2013). These include abiotic factors such as current regime, sedimentation rate, and water chemistry, and biotic factors such as bioerosion, shell mineralogy, community composition, and community growth rates (Posenato et al., 2013). Bivalve beds can also be composed of distinct microstratigraphic units with differing formation processes (Simões & Kowalewski, 1998). Understanding the taphonomy of bivalve beds is crucial to understand the palaeoenvironment (e.g., Fürsich & Pandey, 1999). Bivalves found in oxygen-poor and acidic ocean bottom environments are in some cases interpreted to be death assemblages of pelagic forms, due to the difficulties with shell secretion under reducing conditions (Kurihara, 2008; Hofmann et al., 2010; Fitzer et al., 2014). Mesozoic bivalve beds are known worldwide (e.g., Noe-Nygaard et al., 1987; Conti & Monari, 1992; Fürsich & Pandey, 1999; McRoberts, 2011; Di Stefano et al., 2012; Posenato et al., 2013), but little work has so far been published from the Svalbard archipelago. The Middle Triassic Botneheia Formation in Svalbard was historically known as the "*Daonella* Shales", and the large number of bivalve shells is thought to have contributed significantly to the calcite content of the formation (Mørk et al., 1982). The occurrence of fossil-rich beds in highly organic-rich shales has been considered a tell-tale sign that mass mortality events were frequent (e.g., Krajewski, 2008). Yet, no study has focused on the taphonomy of these beds.

Epifauna of the Boreal region in the Early–Middle Triassic

Daonellids are epibenthic bivalves that are adapted to soft, soupy substrates in dysoxic environments (Wignall, 1993; Schatz, 2005). The genus *Daonella* includes a plethora of described species, often with a high degree of taxonomic uncertainty (McRoberts, 2000, 2010; Schatz, 2001, 2004); see also unpublished work by Bakke (2017). The taxonomy is complicated by the fact that many daonellids lack distinct characters, are poorly preserved, change through ontogeny and/or show wide morphologic variation, and are therefore not determinable based on uni- or bivariate methods (Schatz, 2001, 2004), and that new species are still being described (e.g., Chen & Stiller, 2010). The coquina beds of the *Daonella* shales were described as *Daonella degeeri* by Frebold (1951). Contemporaneous *Daonella frami* (Kittl, 1907) coquina beds were described from Arctic Canada (Tozer, 1961), and Tozer & Parker (1968) suggested that *D. frami* may be a junior synonym of *D. degeeri.* However, Campbell (1994) argued that the more numerous costae and larger maximum size in *D. degeeri* than in *D. frami* is a distinguishing feature, and *D. frami* is still used in recent Boreal Triassic biostratigraphy (McRoberts, 2010; McRoberts et al., 2021). The biostratigraphically used Boreal species include (from oldest to youngest) *Daonella americana, Daonella dubia, Daonella lindstroemi, D. frami* and *Daonella subarctica* (McRoberts, 2010). Campbell (1994) erected the small (<3 mm) *Daonella haraldi,* but it has not been identified in Svalbard since.

Other bivalves have also been recognised from the Middle Triassic of Svalbard. Weitschat & Lehmann (1983) wrote that the bivalve genera *Nucula, Adontophora* and *Gervilleia* are rare in the Triassic rocks on Svalbard but provided no additional information on these finds. Other workers reporting these genera include von Mojsvár (1886) who described *Nucula elongata* in the fauna of the "*Daonella*-Kalk", together with *Daonella lindstroemi* and *Daonella arctica*. Buchan et al. (1965) found *Adontophora* sp. together with *Daonella frami* and *Halobia zitteli*; however, Hounslow et al. (2008) described *Adontophora* sp. together with *Claraia stachei* in the Lower Triassic. Brachiopods have also been mentioned from Lower Triassic (Pchelina, 1977; Wignall et al., 1998) and Middle Triassic rocks (Egorov & Mørk, 2000; Nakrem et al., 2008), but have currently not been described in detail.

Dysoxic tolerance

In the Early Triassic, certain benthic bivalve species tolerated decreased oxygen and increased hydrogen sulphide levels such that they dominated their environment (Bottjer et al., 2008). Etter (1995) described how opportunistic species can reach high abundances in an otherwise low-diversity ecosystem under dysoxic conditions. Aberhan & Baumiller (2003) showed that epifaunal bivalves suffered less than infaunal bivalves during Early Jurassic anoxic episodes. Schatz (2005) argued that *Daonella* could have survived in dysoxic environments. Modern, anaerobically adapted bivalves can survive anoxia for a couple of months (at temperatures of 15–20°C), and species probably had opportunistic life history strategies to cope with this also in the past (Oschmann, 1991). Oschmann (1991) also suggested that *Daonella* could have reached maturity in less than a year and survived in their planktonic larval stage during the anoxic periods.

Oxygen-requiring trace fossils

In addition to bivalves, the trace fossil *Thalassinoides* Ehrenberg, 1944 frequently occurs throughout the Botneheia Formation, and in places covers large areas (Fig. 5B). *Thalassinoides* are burrows that became passively filled after use (Carvalho et al., 2007; Gingras et al., 2011; Yanin & Baraboshkin, 2013). They are characterised by both straight and angled horizontal tunnels of variable size, sometimes with a thin wall lining preserved, and connected to vertical cylindrical shafts (Yanin & Baraboshkin, 2013). The burrows form irregular bulbs at bifurcation points (Yanin & Baraboshkin, 2013). Although rare, body fossils can sometimes be preserved, which have identified the trace maker of *Thalassinoides* to be a crustacean decapod (Sellwood, 1971; Carvalho et al., 2007). *Thalassinoides* burrows are found in well-oxygenated environments and are considered important oxygen indicators (Carvalho et al., 2007; Gingras et al., 2011; Yanin & Baraboshkin, 2013).

Geological setting

Svalbard is an archipelago at 74 to 81 degrees north at the northwestern edge of the Barents Sea, which in the Triassic formed part of the Boreal Sea north of the Pangea continent (Fig. 1). The Boreal Sea was a large outer-shelf embayment at approximately 45°N palaeolatitude which opened into the Panthalassa Ocean. The depositional environment in the Early and Middle Triassic was a coastal to open-marine epicontinental basin, and the resulting dark shales, mudstones and siltstone beds known as the Sassendalen Group are today cropping out on the islands Spitsbergen, Barentsøya, Wilhelmøya, Edgeøya and Bjørnøya (Mørk et al., 1982). The Sassendalen Group in eastern Svalbard is divided into the Lower Triassic Vikinghøgda Formation and the Middle Triassic Botneheia Formation (Mørk & Bjorøy, 1984; Mørk et al., 1999; Vigran et al., 2014). Above lie the prodelta, sideritic purple shales of

the Tschermakfjellet Formation, part of the Kapp Toscana Group (Mørk et al., 1999; Vigran et al., 2014). During the Middle Triassic, the shallow-marine Bravaisberget Formation was deposited in the west and the offshore marine Botneheia Formation in the central and eastern parts of Svalbard (Mørk et al. 1982; Krajewski et al. 2007). The Botneheia Formation was deposited under lower sedimentation rates and is highly enriched in organic material. Numerous studies have focused on the sedimentology as an onshore analogue to potential source rocks in the Barents Sea (e.g., Mørk et al., 1982; Mørk & Bjorøy, 1984; Leith et al., 1993; Mørk et al., 1993; Riis et al., 2008; Vigran et al., 2008; Lundschien et al., 2014; Wesenlund et al., 2021, 2022). Infrastructure on Svalbard makes outcrops relatively easily accessible, and the fossil-rich Botneheia Formation has been extensively studied since the beginning of the last century (e.g., Heuglin, 1874; Dames, 1895; Kittl, 1907; Nathorst, 1910; Wiman, 1916). Since then, the fauna has received less attention, despite an increased interest in global Middle Triassic marine recovery after the end-Permian extinction (e.g., Chen & Benton, 2012; Benton et al., 2013; Lau et al., 2016; Song et al., 2018).

This studied section covers the fossil-rich, black shales and mudstones of the upper part of the Blanknuten Member of the Botneheia Formation (Fig. 2). A transgression in the early Anisian led to an offshore shelf and likely anoxic depositional environment throughout the lower Muen Member, while conditions appear to have fluctuated more in the Ladinian part of the Blanknuten Member (Mørk & Bjorøy, 1984; Krajewski, 2008; Vigran et al., 2014). The formation is commonly carbonate-cemented and interbedded with siltstones of storm origin (Mørk et al., 1982). Phosphate nodules are found throughout the interval, either dispersed in the shale or mudstones or as basal lags in the siltstone (Mørk et al., 1982; Krajewski, 2008). Differentiating phosphate-cemented *Thalassinoides* burrows from microbial-induced phosphate nodules has been a topic of debate (see discussion in Krajewski, 2000 and Mørk & Bromley, 2008).

Materials and methods

Data availability

All samples used in this study are housed in the collections of the Natural History Museum in Oslo, University of Oslo and are readily available for study upon request. PMO = The Palaeontological Museum in Oslo (presently: the Natural History Museum, University of Oslo).

Field site

Fieldwork was conducted in 2018 on the Muen Mountain (77°49’24.2”N, 21°22’39.4”E, 118 m a.s.l.) on Edgeøya, Svalbard (Fig. 1). The logged section is 32.5 m thick, with the Muen plateau (Fig. 3) from 14.7 m to 15.95 m (125 cm vertical thickness). The logged section covers the upper 28.1 m of the Blanknuten Member which at this locality is 41 m thick (Krajewski, 2008). The Muen plateau is approximately 500 metres long, 40–70 metres wide, with horizontal bedding planes (Fig. 3). It is exposed stepwise, and bedding surfaces can therefore be studied laterally for several metres. Bulk shale samples were collected for geochemistry every 1 m throughout the section, and approximately every 5 cm across the Muen plateau (101 samples in total; 27 of these were from the Muen plateau). In order to obtain unweathered material, sampling sites were excavated into the cliffside where possible. Trace fossils and body fossils were collected throughout the section and laterally along the beds, 128 samples in total, and 74 of these from the Muen plateau. Bivalve fossils were usually flattened; these were wrapped in aluminium foil for protection.

Taphonomic analysis of bivalves

Two vertically oriented thin-sections were prepared from *Daonella* bed 1 (DB 1), one from *Daonella* bed 2 (DB 2) and one from the microcoquina bed.

We tested whether the height/width ratio of the collected bivalves could be used to group them into morphotypes. We therefore measured the height and width of 68 bivalves from the section using a calliper; 66 specimens were complete enough to calculate a height/width ratio and of these, 23 were 100% complete (Electronic supplement 1, Table S1). Height was measured as the distance from the umbo to the distalmost point on the ventral margin. No specimens had asymmetrical umbos. Width was measured as the distance from the umbo to the distalmost point of the hinge line. Only one side was measured as few specimens had the complete hinge line preserved. Only bivalves larger than 5 mm in any dimension were included due to the increased relative error margin in smaller specimens. The bivalves come from five intervals: at 1.5 m (11 specimens), 5–6 m (nine specimens), 7.5 m (one specimen), 8.4 m (one specimen) and 14.9–15.5 m (46 specimens). Specimens in DB 1–3 were too fragmented to be measured. Convex-up or down preservation was noted. Completeness was estimated in per cent. We statistically tested the number of morphotypes by Mixture analysis and the Akaike Information Criterion (AIC) in PAST 3.24 (Hammer et al., 2001). AIC measures model fit with a penalty for the number of parameters; the model with the lowest value is desirable.

Shell orientation was measured for the *Daonella* beds and the shale beds in between (Electronic supplement 1, Table S2). Many specimens were lacking the umbo, and to increase the number of measurements, orientation of specimens was measured along the medial axis in 180 degrees. Shell orientations were measured on field pictures using the angle tool in ImageJ v1.52o (Rueden et al., 2017) with the Fiji package (Schindelin et al., 2012). Significance was determined using Rayleigh's test of uniform distribution. We considered $p < 0.05$ as significant.

Oxygenation proxies

Handheld X-Ray fluorescence spectroscopy (HHXRF) was conducted on rock and fossil samples using a Thermo Fisher Scientific Niton XL3t GOLDD+ Analyzer with an 8 mm aperture. Measurements were done on uncrushed samples that had been rinsed with water and dried. The Mining Cu/Zn testing mode was used with an integration time of 90 s (Electronic supplement 1, Table S3).

Thirty-eight samples were analysed for total organic carbon (TOC), C and N. Ground, de-calcified and dried samples were sealed within a Sn bucket and analysed by 1020°C combustion on a Flash 2000 Organic Elemental Analyzer coupled to a Thermo Scientific MAT 253 stable isotope ratio mass spectrometer at the stable isotope geochemistry laboratory at the Open University, UK. Results were calibrated using repeated measurements of in-house reference solutions and international standards (IAEA-Sucrose, L-alanine and L-glutamic acid). Repeated measurements gave a standard deviation of less than 1 for each of these standards.

Pyrite framboid analysis

Pyrite framboids were imaged from eight thin-sections and one rock sample taken from between 14.25 m and 15.31 m (Electronic supplement 1, Table S4). A Variable Pressure Hitachi S–3600N Scanning Electron Microscope (SEM) was used, equipped with a backscattered (BSE) electron detector and a Bruker XFlash® 5030 energy dispersive X-ray detector (EDX) at the Natural History Museum in Oslo. The software used was Esprit 1.9. Analyses were conducted in low vacuum mode (10-–15 Pa) and the

acceleration voltage was 15 kV. We measured pyrite framboids using the circle tool in ImageJ v1.52o (Rueden et al., 2017) with the Fiji package (Schindelin et al., 2012). The diameter was calculated from the area and normalised to the scale in each image.

Results

The benthic fauna in the Muen section consists of a few bivalve taxa and *Thalassinoides*, with single occurrences of *Planolites* and *Rhizocorallium*. Small specimens that could potentially be brachiopods were identified but not determined. Pelagic organisms identified in this study include shark teeth, ichthyosaurs (mixosaurids and cymbospondylids), orthoconic nautiloids and ammonoids.

Lithological description

In our measured 32.5 m of the Botneheia Formation (Fig. 2), the lower 9 m of the section consist of organic-rich, fissile shales interbedded with dolomitic siltstone beds and phosphate nodule conglomerates. The siltstone beds form prominent, calcite-cemented to dolomitic, yellow-weathering benches with current ripple marks. The top surfaces are commonly undulating, likely due to low deposition rates and burrowing of *Thalassinoides*. The preservation of ripples with bioturbation only at the top suggests fast deposition through storms. From 9 m and until 16.5 m, the section consists of thinly laminated, organic-rich paper shale. Phosphate occurs throughout as phosphate nodules (dispersed) or as infill in *Thalassinoides* burrows (connected tunnels). The upper part of the Botneheia Formation consists of grey, thinly laminated fissile shales with flattened phosphate nodules. The formation boundary at 28.1 m marks the regression between the basinal Botneheia Formation and the Tschermakfjellet Formation, which was deposited in a prodelta setting with greyish to purple shale, without any calcitic cement, but orange to reddish siderite nodules are common.

Taphonomy

The Muen section offers large bedding planes, with both body and trace fossils such as *Daonella* beds (DB 1–3) (Fig. 5A), *Thalassinoides* burrows (Fig. 5B), disarticulated and semi-articulated ichthyosaur remains (Fig. 5C–D), and possible microbial mat structures (resembling “elephant skin” and “bubble marks”, Fig. 5E–F). *Daonella* beds are exposed at 15.1 m (DB 1), 15.2 m (DB 2) and 15.3 m (DB 3) in the section (Fig. 4). Additionally, narrow horizons with accumulation of small (<1 mm) bivalves were identified at 8.9 m, 14.25 m and 14.9 m. The DBs are monospecific and consist mainly of shells and little matrix (Fig. 6), occasionally pyritised. The shells both in the DBs, and in the shale beds in between, are preserved as completely flattened, calcitic single valves. No imbrication was observed. All DBs rest on sharp, erosional surfaces, as described by Kidwell (1986) for shell bed Type IV. This reflects a change from negative to either zero (omission), or positive (deposition) values (Kidwell, 1986, p. 10). Kidwell (1986) introduced a formation model for shell beds where the dynamics between hard-part input (shell supply) and net sedimentation, control the density of hard-part preservation. The shell packing density does not diminish in the DBs, however, and is therefore representative of zero (omission) values throughout the beds, and not positive (deposition) values. Unlike the model for Type IV (an increase in sedimentation leads to a decrease in shell density) proposed by Kidwell (1986, fig. 2), the DBs contain a pure fossil concentration throughout, and end with zero (omission) surfaces similar to Type I shell beds (DB1–2) or negative (erosion) surfaces similar to Type III shell concentrations (DB 3). The upper boundary of DB 3 undulates markedly, and the surface is covered in *Thalassinoides*

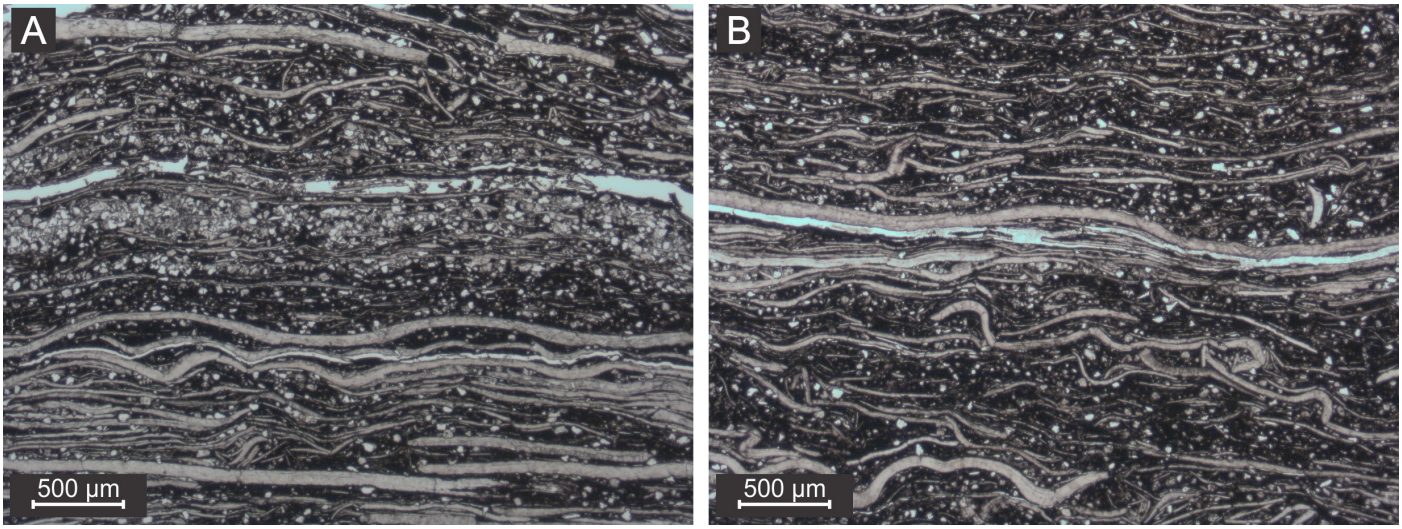

Figure 6. Photomicrographs in grey scale of Daonella *beds in thin-section using transmitted light. (A) Sample PMO 234.168 from DB 1. (B) Sample PMO 234.171 from DB 2.*

burrows that appear to have burrowed into the shell concentrations. It was not possible to estimate other changes in the intensity or frequency of post-mortem destruction between or throughout the DBs. Some of the shells in DB 1 and 2 are slightly deformed in thin-section, possibly from early burial deformation (compaction). DB 1 and DB 2 exhibit distinct orientation of shells (highest Rayleigh's p value = 0.0048 and R = 0.26), while DB 3 shows less pronounced orientation, possibly due to the burrowing (Fig. 4; Electronic supplement 1, Table S2). The bivalve shells between DB 1 and DB 2 also show strong orientation (p = 4 x 10^{-5}, R = 0.39). No significant orientation is seen in the specimens between DB 2 and DB 3 (p = 0.32, R = 0.11) or above DB 3 (p = 0.91, R = 0.04).

Bivalve taxa

The bivalve specimens in the study are poorly preserved, and the taxonomic division is therefore uncertain. Although calcitic shells are often preserved in the DBs, the bivalves are mainly preserved as moulds of single valves in the other parts of the logged section. The bivalve specimens are divided into four taxa: *Daonella*, cf. *Aparimella,* a nuculid and a bakevelliid possibly belonging to the genus *Gervilleia* or *Bakevellia.* Additionally, *Halobia* sp. was identified in the Tschermakfjellet Formation, but not sampled. Two species of *Daonella* were identified: *Daonella degeeri* has radial ribs covering the entire valve, no auricle, is relatively large (>5 cm), with a straight hinge line. The ribs are tightly spaced. *Daonella frami* is smaller and has fewer and broader costae. A specimen of *Daonella* cf. *lindstroemi* was found at 1.5 m. It has radial ribs that flare strongly laterally, but the specimen is fragmented and cannot be confidently determined. *Daonella* was found in four horizons (1.5 m, 5.9 m, 14.9 m, 15 m), and in and in between the beds DB 1–3. The nuculid was identified based on the small size (<1 cm), strong convexity, lack of radial ribs or auricle, and the presence of weak comarginal growth lines. Specimens were found in four horizons (5.6 m, 5.9 m, 14.9 m and 15.5 m). Two bakevelliid specimens were identified based on being strongly inequilateral, concentric growth lines, the lack of ribs and strongly convex shape. These were found in silty horizons 5.2 m and 5.9 m. cf. *Aparimella* was identified based on being taller than wide, equilateral, with radial ribs which bifurcate in larger specimens, concentric growth lines, the presence of a small auricle, and a straight hinge line. Early growth stage specimens are small and inflated, resembling those described for *Aparimella rugosoides* by Campbell (1994). The larger specimens, however, are not as elongate as *A. rugosoides*, and the higher than long shape of the larger specimens is similar to *Halobia*. The studied specimens

lack, however, the byssal tube. The shorter hinge than shell width is shared by *Aparimella beggi* from New Zealand (Campbell, 1994). Cf. *Aparimella* was identified in five horizons (1.5 m, 2.6 m, 5.1 m, 7.5 m and 15 m). The siltier beds contained a greater richness in species than the black shale intervals.

Morphotype analysis

We attempted to determine bivalve morphotypes based on height/width ratios (Electronic supplement 1, Table S1) using the Akaike Information Criterion, in order to test whether this was a feasible way of quickly grouping the bivalve specimens. AIC is lowest for four morphotypes (AIC = - 44.82) with height/width ratios of 0.6, 1.0, 2.5 and 4.7, but the number of groups varied between two and four, indicating that the support for either model was low (Fig. S1). *Daonella* in differing stages of ontogeny plotted as two groups (with ratios 0.6 and 1.0) in two of the three outcomes. This concurs with the findings by Schatz (2001, 2004) on the subgenus *Daonella (Arzelella)*, showing that the height/width ratio of tyrolensiform daonellids changes through ontogeny. Also, the nuculids fall within the same group as *Daonella.* The stratigraphic intervals with the highest number of specimens also show the most variation in specimen size, so no link between living conditions and growth can be established.

Bivalve preservation as butterfly preservation (both valves articulated but folded out) is seen in eight *Daonella* specimens: six at 1.5 m, one at 15 m and one at 15.3 m (directly above DB 3). Butterfly preservation was not possible to observe in the DBs due to poor preservation. Butterfly preservation suggests short transport distances, if any (Oschmann, 1991). Especially DB 3 is poorly preserved with shells partly dissolved. All DBs are partly pyritised, which is also seen in the Lower Oxford Clay, where shell beds acted as aquifers for sulphide-rich fluids (Duff, 1975). All bivalve specimens in the study are flattened, except eight single valve specimens that are preserved three-dimensionally (two *Daonella*, four cf. A*parimella* and the two bakevelliids). These are found in seven levels: in the siltier interval from 5.1 m to 5.9 m (three cf. *Aparimella,* two bakevelliids) and in the shale sequences: 8.4 m (one cf. *Aparimella*), 15.2 m (one *Daonella*) and 15.5 m (one *Daonella*). Three-dimensional preservation is more likely in the bakevelliids (2 of 2 specimens) and cf. *Aparimella* (4 of 11 specimens) than in *Daonella* (2 of 53 specimens). One-third of the shells (17 of the 37 specimens that could be determined) were lying convex-down, while the remaining 2/3 were preserved convex-up (not significantly different from random; binomial test, $p = 0.62$).

Trace fossils

Phosphate-filled *Thalassinoides* burrows are found at regular intervals irrespective of lithology, including one occurrence of *Planolites* at 3.4 m. *Thalassinoides* burrows are several cm wide and are easily recognisable in the field (Fig. 5B). In the best exposed part of the section, from 14.2 to 16.1 m, we observed 23 horizons with *Thalassinoides* burrows. These were easily distinguishable from phosphate nodules on the bedding surfaces as they show a high degree of connectivity. In many of the beds, they cover between 50 and 80% of the surface area, with mainly Y-pattern branching (Fig. 5B). *Thalassinoides* can be hard to differentiate from phosphate nodules in vertical sections. We observed several beds of only disconnected phosphate nodules, thought to have been caused by winnowing. Mørk & Bromley (2008) observed *Chondrites* burrows to cross-cut or infill *Thalassinoides* in Middle Triassic strata in Central Spitsbergen. Surprisingly, *Chondrites* was not observed in this study.

Microbial mats

Wavy surfaces resembling wrinkle structures, and pitted surfaces resembling bubble marks were seen on certain shale surfaces (Fig. 5E–F). The structures were found in beds without any bivalves or trace fossils and are interpreted as microbial mats. Similar structures as depicted in Fig. 5E have also been described as palimpsest structures by Chu et al. (2017, fig. 7 c–d) and as bubble structures by Wignall et al. (2020).

Framboidal pyrite

Pyrite framboids were present in all eight thin-sections and the rock sample. Most samples have a size variation within the lower to upper dysoxic range (Bond & Wignall, 2010), including DB 2 and DB 3 (Electronic supplement 1, Table S4). DB 1, however, has small framboids with a narrow size range (mean diameter 5.2 µm, standard deviation 1.7 µm, n = 65), typical of lower dysoxic to anoxic environments (Fig. 7) (Bond & Wignall, 2010). A sample from 4 cm above DB 3 also indicates anoxic conditions.

Geochemical proxies

Elemental redox proxies and the calcium content were plotted against the stratigraphy (Fig. 8; Electronic supplement 1, Table S3). Deposition fluctuates between carbonates and siliciclastics, probably due to the variations in sediment input (Fig. 8A). Two such elements are V and Mo (Morford et al., 2001). These were added and normalised over Al to correct for the effect of increased clay mineral content in the lithologies. The ((V + Mo) * 1000) / Al-curve corresponds well to the oxygenation level indicated by the pyrite framboids and to the presence of trace fossils. The ((V + Mo) * 1000) / Al-curve fluctuates across the Muen plateau, supporting strong time-averaging caused by low rates of deposition (Fig. 8B).

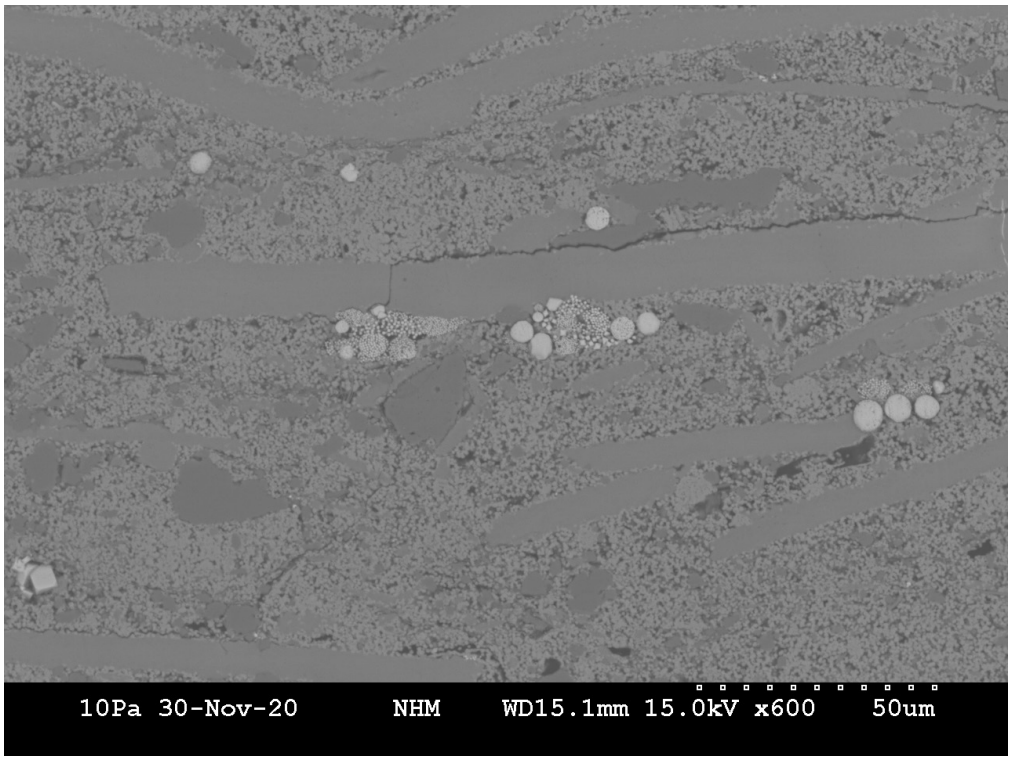

Figure 7. PMO 234.168. Pyrite framboids from DB 1 observed in a scanning electron microscope (SEM) using backscattered electron mode (BSE). Pyrite framboids are common and have a relatively narrow size range. The presence of some crystalline pyrite is typical for lower dysoxic environments.

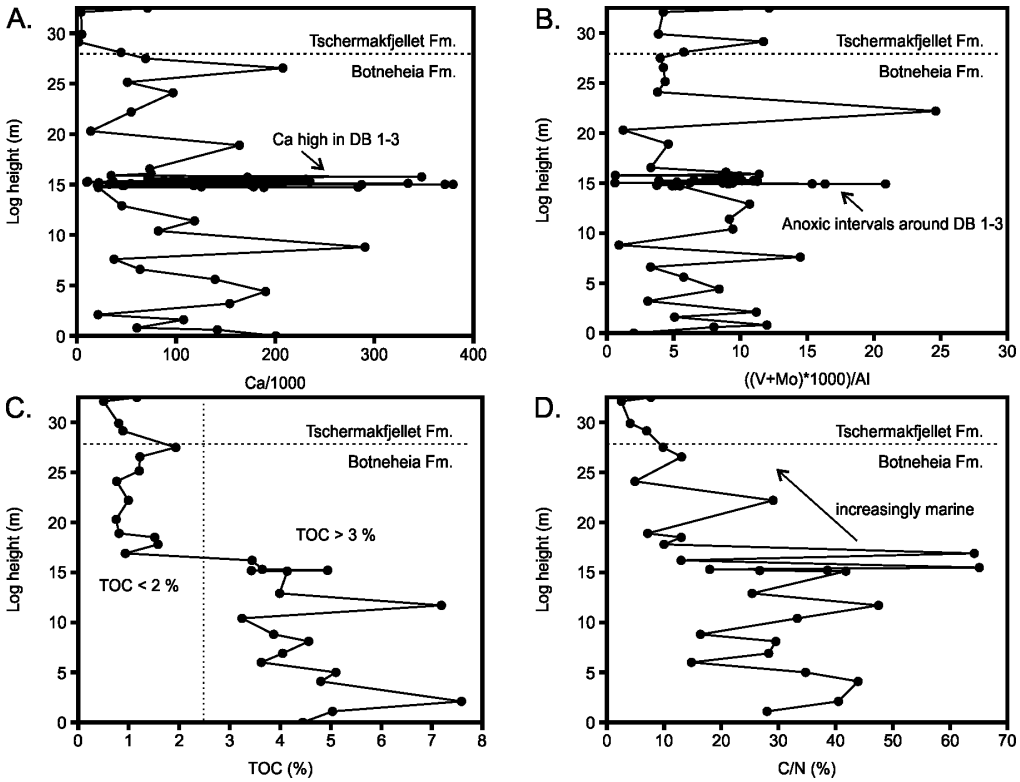

*Figure 8. Geochemical proxies plotted against the stratigraphy. (A) Calcium content. (B) ((V + Mo) * 1000) / Al-curve, high values indicate dysoxic to anoxic values. (C) Total organic carbon (TOC). (D) C/N ratio, lower values indicate terrestrial organic input, while higher values indicate marine and algal organic input.*

Organic matter

The section can be divided into two units based on total organic carbon (TOC): a lower interval with high TOC (0–16.5 m) and an upper interval with low TOC (16.5–32.5 m, including the Tschermakfjellet Formation) (Fig. 8C). The mean TOC is 4.5% (3.2–7.6%, n = 19) in the lower part, and 1% (0.5–1.9%, n = 14) in the upper. The C/N ratio can indicate the origin of sedimentary organic material, such as whether it originated from algae or vascular plants (e.g., Meyers, 1994; Sampei & Matsumoto, 2001; Lamb et al., 2006). Algae have no cellulose, and typical C/N ratios are 4–10, while vascular plants with cellulose have C/N ratios above 20 (Meyers, 1994). The C/N ratio shows that the organic content was a mix of terrestrial and marine in the lower half of the studied section, then increasingly marine (Fig. 8D). There is a distinct shift in the origin of organic material between 16.9 m (C/N ratio 64.2) and 17.8 m (C/N ratio 10.0) (Fig. 8D). Between 0 m and 16.9 m, the mean (range) of the C/N ratio is 33.9 (3.96 to 64.2, n = 18). In the interval 17.8–28.1 m, all values are in the marine range with a mean of 12.4 (4.90–15.1, n = 7). The Tschermakfjellet Formation has lower values with a mean of 5.31 (2.53–7.69, n = 4), indicating an algal origin (Meyers, 1994; Lamb et al., 2006).

Discussion

Both palaeontological and other oxygenation indicators vary significantly over short stratigraphic intervals, supporting our interpretation that the environment was characterised by rapid fluctuations in oxygen levels. This provides a more nuanced model than previously suggested, explaining how bivalve beds with oriented shells, beds with burrowing, oxygen-requiring crustaceans, and anoxic shale beds devoid of benthic life, could form within relatively short intervals. Krajewski (2008) considered *Daonella* to be possibly planktonic, and therefore interpreted the shell beds in the Botneheia Formation as a result of mass mortality events caused by toxic pulses of hydrogen sulphide. However, the accumulation of shells from a mass mortality event is a contradiction. An instantaneous cessation of shell production would lead to a decreased shell density in the sediment, not an increase.

Daonella outcompeted during more oxygenated episodes

The bivalve fauna in the Muen section is unevenly distributed, and the specimen-richest intervals (excluding the monospecific DBs) also show the highest species richness and size variation. *Daonella* was found throughout the section, but cf. *Aparimella* is common in the lower, siltstone-rich interval. *Daonella* became the dominating taxon after a shift in deposition towards organic-rich paper shales. Bakevelliids (probably semi-infaunal, byssally attached suspension feeders) were only found in silty shale at 5.15 m and in a siltstone bed with ripple marks at 5.9 m, when increased current velocities led to more favourable conditions for more oxygen-requiring species. Only one *Daonella* was found in this bed, possibly because daonellids were outcompeted during periods of increased oxygenation, that they required a softer substrate, and/or possibly because their thin shells had lower preservation potential in a higher-energy regime.

Bivalve beds formed by winnowing

The shell concentrations (DBs) have lower bed contacts similar to those described for Type IV by Kidwell (1986), reflecting “an increase in net sedimentation rate from negative (erosion) values through zero (omission) surfaces to positive (deposition) values” (Kidwell, 1986, p. 10). However, the top surfaces of DB and DB2 appear to be of Type I defined by Kidwell (1986); “a shell pavement that record the final stage of zero net sedimentation (sedimentary omission)”, or for DB 3: Type II with low sedimentation rates and winnowing. This explains how the shells in DB 1 and DB 2 show a preferred orientation in plan view, but DB 3 less so, as the bed was extensively burrowed by *Thalassinoides* during the erosional phase. The observed upwards reduction in preferred orientation in the bivalve beds and the beds between and above them, is thought to have been caused by a reduction in the deep-water currents responsible for causing the shell orientation. Microbial structures were found in intervals lacking benthic body or trace fossils (Fig. 4), indicating that they formed during anoxic events. Open marine microbial mats have been described from the Lower Triassic in the Sverdrup Basin in Arctic Canada, where they occur under reducing conditions in the photic zone (Wignall et al., 2020). Algal blooms can cause decomposing biofilms on the sediment surface, protecting the substrate against erosion, and importantly, microbial structures can be misidentified for sedimentary structures such as palimpset ripples (Davies et al., 2016). However, we consider it unlikely to have several generations of intersecting ripple marks preserved in a black shale sequence (such as the structures seen in Fig. 5E).

Krajewski (2008) suggested that oxygen deficiency or toxic pulses of hydrogen sulphide could have caused mass-mortality events, and thereby produced the fossiliferous beds. However, the fauna is composed of both dysoxia-tolerant *Daonella*, and air-breathing ichthyosaurs (e.g., Maxwell & Kear,

2013; Hurum et al., 2014; Økland et al., 2018; Roberts et al., 2022); air-breathing vertebrates would not have been affected by the oxygen deficiency. The Botneheia Formation was deposited in a basinal setting, with low sedimentation rates and high organic input from the overlying water masses (Mørk et al., 1982). We suggest that deep-water currents were responsible for the orientation and erosive bases of the bivalve shells, and for providing the oxygenation required for *Thalassinoides* to regularly colonise the sea floor throughout the muddy interval. The *Thalassinoides* burrows in siltstone beds may have been initiated by storm events causing temporarily increased oxygen levels. We believe that the combination of high organic input (as reflected in that the high TOC values in the lower half of the section correspond to the fossil richness in this interval) and low sedimentation rates led to a high preservation potential, rather than mass-mortality events. The DBs are several cm-thick accumulations of compacted shells. If they had represented living communities that were quickly deposited after mass death events, an initial living bivalve thickness and abundance would have been necessary that we consider improbable for a community at a single point in time. Also, to identify a mass-mortality event, the accumulation and/or preservation rate of the organisms must be increased. Killing all bivalves in an area at a given moment in time would not increase the total number of preserved bivalves. After episodes of mass mortality, the affected organism would occur in reduced numbers in the overlying strata. This is, however, hard to observe in black shales, due to the low deposition rate and high time-averaging.

Taxonomic uncertainty

Daonella frami and *Daonella degeeri* are time-equivalent, occur in the same strata and both form bivalve beds (*D. frami* in Arctic Canada, *D. degeeri* in Svalbard). Consequently, their relationship has been a topic of debate (Tozer & Parker, 1968). In this study, *D. frami* is commonly seen in the beds in between the *D. degeeri*-dominated bivalve beds. Importantly, the specimens in the beds are poorly preserved and mainly fragments of single valves, and must be used with caution taxonomically. We would consider that the differences in size and in the number of ribs could be an adaptation to changes in substrate conditions or other environmental factors. However, more localities and specimens will have to be studied to resolve this.

Another interesting observation is that cf. *Aparimella* was found in the beds below the Muen plateau, and therefore below the main occurrences of *Daonella*. Campbell (1994) considered *Aparimella* to be more derived than *Daonella* (due to the presence of an auricle), but not as derived as *Halobia* (with a byssus tube), naming it “an intermediate evolutionary step” (Campbell, 1994, p. 65). We consider this model too simplified, as all three genera occur within short timespans (late Ladinian–early Carnian) around the globe, each with multiple endemic species. The taxonomic division of *Daonella, Aparimella* and *Halobia* has also been discussed by McRoberts (2000), arguing for a polyphyletic origin of *Halobia.* Occurrences of cf. *Aparimella* below the DBs contradict the notion that cf. *Aparimella* is a derived form of *Daonella*.

Sediment oxygenation

Horizontal *Thalassinoides* burrows are common in the lower half of the section. No vertical shafts or tiering structures were seen, possibly as vertical traces would be flattened by compaction. The horizontal tunnels and branching are well preserved. The shallow burrowing and lack of tiering suggests poorer living conditions deeper in the soupy sediment (Martin, 2004; Gingras et al., 2011). It could also indicate too short a period of oxygenation to establish a tiering structure (Savrda & Bottjer, 1989; Martin, 2004). Mørk & Bromley (2008) described well-preserved tiering structures in the Middle Triassic on western Spitsbergen, in a siltstone-dominated succession. The authors referred eastern

Svalbard to the *Thalassinoides* ichnofacies assemblage. In their only log from eastern Svalbard at Høgrinden in Barentsøya (~ 50 km north of this study), however, only *Thalassinoides* was identified. No other ichnogenera were identified in this study, suggesting that the low diversity is regional in eastern Svalbard.

Phosphate accumulations

Certain horizons in the lower half of our logged section, and almost the entire upper half of the section, are fossil poor. This is thought to be due to a gradual reduction in habitability and to the prevailing euxinic conditions described for the Blanknuten Member (Krajewski, 2008). The reduction in shell orientation from the beds below DB 1, up to the beds above DB 3, indicate a reduction in bottom currents. This could have contributed to the stagnant bottom waters. An upward reduction in current velocities is also supported by the trend in ichthyosaur preservation in DB 1–3: from mostly disarticulated material (DB 1, the exception is PMO 219.250, see description in Hurum et al. 2014) to strings of vertebrae (DB 2) and more articulated specimens (DB 3). Very little sediment matrix is seen in the thin-sections of DB 1 and 2, as would be expected for shell accumulations formed by winnowing and very low rates of deposition. The Botneheia Formation is thinner in eastern Svalbard compared with western Spitsbergen (Mørk et al., 1982; Mørk & Bjorøy, 1984), and the lower depositional rates could cause higher phosphate levels due to precipitation from sea water. Phosphate accumulations are also believed to be caused by winnowing (Krajewski, 2008), supported by the fact that the upper part of the section contains little phosphate. Mørk & Bromley (2008) argued that phosphate nodules originated from infilled burrows, while Krajewski (2008) stated that there was no correlation between the two in the Eastern areas. The large lateral exposures in this study made it possible to differentiate between individual phosphate nodules and phosphatised *Thalassinoides* burrows. We support winnowing or storm erosion as the driving mechanism behind the primary phosphate lags as introduced by Mørk et al. (1982).

Conclusions

The excellent exposure of the Muen Plateau enables detailed investigation of the upper part of the Botneheia Formation on eastern Svalbard. The Muen section records a high fossil richness but a low species diversity, typical for dysoxic and fluctuating environments; an observation also supported by the repeated occurrences of trace fossils. Oxygen deficiency (e.g., by algal blooms) may be the most likely key factor for the high fossil-preservation potential of both the benthic and the pelagic fauna. We thus disagree that mass-mortality events (by oxygen deficiency or toxic pulses of hydrogen sulphide) were the main drivers behind the fossiliferous beds as has previously been suggested. The DBs exhibit preferred orientation of shells and contain only very little and fine sediment, supporting the view that winnowing processes were responsible for their formation.

Acknowledgements. We thank the Editor, Snorre Olaussen and an anonymous reviewer for constructive comments. We also want to thank Dr. Franz T. Fürsich, Dr. Silvia Danise and an unknown reviewer for thoroughly revising an earlier draft of the manuscript. This research was funded by ARCEx partners and the Research Council of Norway (grant number 228107). A special thanks to the Dale Oen Experience for field logistics. All necessary permits were obtained from the Governor of Svalbard for fieldwork in 2018 (RiS 4061).

References

Aberhan, M. & Baumiller, T.K. 2003: Selective extinction among Early Jurassic bivalves: A consequence of anoxia. *Geology 31*, 1077. https://doi.org/10.1130/G19938.1

Allison, P.A., Wignall, P.B. & Brett, C.E. 1995: Palaeo-oxygenation: effects and recognition. *Geological Society, London, Special Publications 83*, 97–112. https://doi.org/10.1144/GSL.SP.1995.083.01.06

Bakke, N. 2017: *The evolution of the Triassic bivalve Daonella into Halobia in the Botneheia Formation on Svalbard*. MSc thesis, NTNU, 185 pp.

Benton, M.J., Zhang, Q., Hu, S., Chen, Z.-Q., Wen, W., Liu, J., Huang, J., Zhou, C., Xie, T., Tong, J. & Choo, B. 2013: Exceptional vertebrate biotas from the Triassic of China, and the expansion of marine ecosystems after the Permo-Triassic mass extinction. *Earth-Science Reviews 125*, 199–243. https://doi.org/10.1016/j.earscirev.2013.05.014

Benton, M.J. 2018: Hyperthermal-driven mass extinctions: killing models during the Permian–Triassic mass extinction. *Philosophical Transactions of the Royal Society A: Mathematical, Physical and Engineering Sciences 376,* 20170076. https://doi.org/10.1098/rsta.2017.0076

Bond, D.P.G. & Wignall, P.B. 2010: Pyrite framboid study of marine Permian–Triassic boundary sections: A complex anoxic event and its relationship to contemporaneous mass extinction. *GSA Bulletin 122,* 1265–1279. https://doi.org/10.1130/B30042.1

Bond, D.P.G. & Grasby, S.E. 2017: On the causes of mass extinctions. *Palaeogeography, Palaeoclimatology, Palaeoecology 478*, 3–29. doi: https://doi.org/10.1016/j.palaeo.2016.11.005

Bottjer, D.J., Clapham, M.E., Fraiser, M.L. & Powers, C.M. 2008: Understanding mechanisms for the end-Permian mass extinction and the protracted Early Triassic aftermath and recovery. *GSA Today 18*, 4–10. https://doi.org/10.1130/GSATG8A.1

Buchan, S., Challinor, A., Harland, W. & Parker, J. 1965: The Triassic stratigraphy of Svalbard. *Norsk Polarinstitutt Skrifter 135*, 1–94.

Byers, C.W. 1977: Biofacies patterns in euxinic basins: a general model. *In* Cook, H.E. & Enos, P. (eds.): *Deep-water carbonate environments 25,* Society of Economic Paleontologists and Mineralogists Special Publication, 5–17. https://doi.org/10.2110/pec.77.25.0005

Böhm, J. 1912: *Über Triasversteinerungen vom Bellsunde auf Spitzbergen*. Kungliga Svenska Vetenskaps-akademien, Almquist & Wiksells Boktryckeri, Stockholm, 1–15.

Campbell, H.J. 1994: The Triassic bivalves Daonella and Halobia in New Zealand, New Caledonia, and Svalbard. *Institute of Geological and Nuclear Sciences Monograph 4*, 1–166.

Carvalho, C., Andrade Viegas, P. & Cachão, M. 2007: *Thalassinoides* and its Producer: Populations of *Mecochirus* Buried within their Burrow Systems, Boca do Chapim Formation (Lower Cretaceous), Portugal. *PALAIOS 22*, 104–109. https://doi.org/10.2110/palo.2006.p06-011r

Chen, J.-H. & Stiller, F. 2010: An early *Daonella* from the Middle Anisian of Guangxi, southwestern China, and its phylogenetical significance. *Swiss Journal of Geosciences 103*, 523–533. https://doi.org/10.1007/s00015-010-0035-z

Chen, Z.-Q. & Benton, M.J. 2012: The timing and pattern of biotic recovery following the end-Permian mass extinction. *Nature Geoscience 5,* 375. https://doi.org/10.1038/ngeo1475

Chu, D., Tong, J., Bottjer, D.J., Song, H., Song, H., Benton, M.J., Tian, L. & Guo, W. 2017: Microbial mats in the terrestrial Lower Triassic of North China and implications for the Permian–Triassic mass extinction. *Palaeogeography, Palaeoclimatology, Palaeoecology 474,* 214–231. https://doi.org/10.1016/j.palaeo.2016.06.013

Clapham, M.E. & Payne, J.L. 2011: Acidification, anoxia, and extinction: A multiple logistic regression analysis of extinction selectivity during the Middle and Late Permian. *Geology 39*, 1059–1062. https://doi.org/10.1130/G32230.1

Conti, M. & Monari, S. 1992: Thin-shelled bivalves from the Jurassic Rosso Ammonitico and Calcari a Posidonia formations of the Umbrian-Marchean Apennine (central Italy). *Paleopelagos 1992*. 193–213

Dallmann, W.K. 2015: Geoscience Atlas of Svalbard. *Norsk Polarinstitutt,* Report Series No. 148, *Tromsø, 978 82 7666-312-9*, 1–292.

Dames, W.B. 1895: Über die Ichthyopterygier der Triasformation. *Sitzungsberichte der Akademie der Wissenschaften zu Berlin 46*, 1045–1050.

Davies, N.S., Liu, A.G., Gibling, M.R. & Miller, R.F. 2016: Resolving MISS conceptions and misconceptions: A geological approach to sedimentary surface textures generated by microbial and abiotic processes. *Earth-Science Reviews 154*, 210–246. https://doi.org/10.1016/j.earscirev.2016.01.005

Di Stefano, P., McRoberts, C., Renda, P., Tripodo, A., Torre, A. & Torre, F. 2012: Middle Triassic (Ladinian) deep-water sediments in Sicily: new findings from the Madonie Mountains. Rivista italiana di paleontologia e stratigrafia 118, 235–246.

Duff, K. 1975: Palaeoecology of a bituminous shale—the Lower Oxford Clay of central England. *Palaeontology 18*, 443–482.

Dustira, A.M., Wignall, P.B., Joachimski, M., Blomeier, D., Hartkopf-Fröder, C. & Bond, D.P.G. 2013: Gradual onset of anoxia across the Permian–Triassic boundary in Svalbard, Norway. P*alaeogeography, Palaeoclimatology, Palaeoecology 374*, 303–313. https://doi.org/10.1016/j.palaeo.2013.02.004

Egorov, A.Y. & Mørk, A. 2000: The East Siberian and Svalbard Triassic successions and their sequence stratigraphical relationships. *Zentralblatt für Geologie und Paläontologie, Teil 1,* 1377–1430.

Ehrenberg, K. 1944: Ergänzende Bemerkungen zu den seinerzeit aus dem Miozän von Burgschleinitz beschriebenen Gangkernen und Bauten dekapoder Krebse. *Paläontologische Zeitschrift 23,* 354–359. https://doi.org/10.1007/BF03160443

Etter, W. 1995: Benthic diversity patterns in oxygenation gradients: an example from the Middle Jurassic of Switzerland. *Lethaia 28,* 259–270. https://doi.org/10.1111/j.1502-3931.1995.tb01430.x

Fitzer, S.C., Cusack, M., Phoenix, V.R. & Kamenos, N.A. 2014: Ocean acidification reduces the crystallographic control in juvenile mussel shells. *Journal of Structural Biology 188,* 39–45. https://doi.org/10.1016/j.jsb.2014.08.007

Frebold, H. 1951: Geologie des Barentsschelfes. *Abhandlungen der Deutschen Akademie der Wissenschaften zu Berlin Jahrgang 1950,* 1–150.

Fürsich, F.T. & Pandey, D.K. 1999: Genesis and environmental significance of Upper Cretaceous shell concentrations from the Cauvery Basin, southern India. *Palaeogeography, Palaeoclimatology, Palaeoecology 145*, 119–139. https://doi.org/10.1016/S0031-0182(98)00099-6

Gingras, M.K., Maceachern, J.A. & Dashtgard, S.E. 2011: Process ichnology and the elucidation of physico-chemical stress. *Sedimentary Geology 237*, 115–134. https://doi.org/10.1016/j.sedgeo.2011.02.006

Grasby, S.E., Beauchamp, B. & Knies, J. 2016: Early Triassic productivity crises delayed recovery from world's worst mass extinction. *Geology 44*, 779–782. https://doi.org/10.1130/G38141.1

Hammer, Ø., Harper, D.A.T. & Ryan, P.D. 2001: Past: Paleontological statistics software package for education and data analysis. *Paleontologia Electronica 4,* 1–9.

Heuglin, T. 1874: Teil 3: Beiträge zur Fauna, Flora und Geologie von Spitzbergen und Novaja Zemlja: *Heuglin, Theodor von (1824–1876). Reisen nach dem Nordpolarmeer in den Jahren 1870 und 1871*., Georg-Westermann-Verlag, Druckerei and Kartographische Anstalt, Braunschweig, 1–352.

Hofmann, G.E., Barry, J.P., Edmunds, P.J., Gates, R.D., Hutchins, D.A., Klinger, T. & Sewell, M.A. 2010: The Effect of Ocean Acidification on Calcifying Organisms in Marine Ecosystems: An Organism-to-Ecosystem Perspective. *Annual Review of Ecology, Evolution, and Systematics 41,* 127–147. https://doi.org/10.1146/annurev.ecolsys.110308.120227

Hotinski, R.M., Bice, K.L., Kump, L.R., Najjar, R.G. & Arthur, M.A. 2001: Ocean stagnation and end-Permian anoxia. *Geology 29,* 7–10. https://doi.org/10.1130/0091-7613(2001)029<0007:OSAEPA>2.0.CO;2

Hounslow, M.W., Peters, C., Mørk, A., Weitschat, W. & Vigran, J.O. 2008: Biomagnetostratigraphy of the Vikinghøgda Formation, Svalbard (Arctic Norway), and the geomagnetic polarity timescale for the Lower Triassic. *Geological Society of America Bulletin 120*, 1305–1325. https://doi.org/10.1130/B26103.1

Hurum, J.H., Roberts, A.J., Nakrem, H.A., Stenløkk, J.A. & Mørk, A. 2014: The first recovered ichthyosaur from the Middle Triassic of Edgeøya, Svalbard. *Norwegian Petroleum Directorate Bulletin 11*, 97–110.

Kidwell, S.M. 1986: Models for fossil concentrations: paleobiologic implications. *Paleobiology 12*, 6–24. https://doi.org/10.1017/S0094837300002943

Kittl, E.A.L. 1907: *Die Triasfossilien vom Heureka Sund.* Report of the Second Norwegian Arctic Expedition in the "Fram" 1898-1902; No. 7. A. W. Brøgger, Kristiania, 44 pp.

Krajewski, K.P. 2000: Phosphogenic facies and processes in the Triassic of Svalbard. *Studia Geologica Polonica 116,* 7–84.

Krajewski, K.P., Karcz, P., Wozny, E. & Mørk, A. 2007: Type section of the Bravaisberget Formation (Middle Triassic) at Bravaisberget, western Nathorst Land, Spitsbergen, Svalbard. *Polish Polar Research 28,* 79–122.

Krajewski, K.P. 2008: The Botneheia Formation (Middle Triassic) in Edgeøya and Barentsøya, Svalbard: lithostratigraphy, facies, phosphogenesis, paleoenvironment. *Polish Polar Research 29*, 319–364.

Krajewski, K.P. 2013: Organic matter–apatite–pyrite relationships in the Botneheia Formation (Middle Triassic) of eastern Svalbard: Relevance to the formation of petroleum source rocks in the NW Barents Sea shelf. *Marine and Petroleum Geology 45*, 69–105. https://doi.org/10.1016/j.marpetgeo.2013.04.016

Kurihara, H. 2008: Effects of CO2-driven ocean acidification on the early developmental stages of invertebrates. *Marine Ecology Progress Series 373*, 275–284. https://doi.org/10.3354/meps07802

Lamb, A.L., Wilson, G.P. & Leng, M.J. 2006: A review of coastal palaeoclimate and relative sea-level reconstructions using δ13C and C/N ratios in organic material. *Earth-Science Reviews 75,* 29–57. https://doi.org/10.1016/j.earscirev.2005.10.003

Lau, K.V., Maher, K., Altiner, D., Kelley, B.M., Kump, L.R., Lehrmann, D.J., Silva-Tamayo, J.C., Weaver, K.L., Yu, M. & Payne, J.L. 2016: Marine anoxia and delayed Earth system recovery after the end-Permian extinction. *Proceedings of the National Academy of Sciences 113*, 2360–2365. https://doi.org/10.1073/pnas.1515080113

Leith, T.L., Weiss, H.M., Mørk, A., Århus, N., Elvebakk, G., Embry, A.F., Brooks, P.W., Stewart, K.R., Pchelina, T.M., Bro, E.G., Verba, M.L., Danyushevskaya, A. & Borisov, A.V. 1993: Mesozoic hydrocarbon source-rocks of the Arctic region. *In* Vorren, T.O., Bergsager, E., Dahl-Stamnes, Ø.A., Holter, E., Johansen, B., Lie, E. & Lund, T.B. (eds.): *Arctic Geology and Petroleum Potential, Norwegian Petroleum Society Special Publication 2,* Elsevier, Amsterdam, 1–25. https://doi.org/10.1016/B978-0-444-88943-0.50006-X

Lundschien, B.A., Høy, T. & Mørk, A. 2014: Triassic hydrocarbon potential in the Northern Barents Sea; integrating Svalbard and stratigraphic core data. *Norwegian Petroleum Directorate Bulletin 11*, 3–20.

Lyons, T.W. & Severmann, S. 2006: A critical look at iron paleoredox proxies: New insights from modern euxinic marine basins. *Geochimica et Cosmochimica Acta 70*, 5698–5722. https://doi.org/10.1016/j.gca.2006.08.021

MacQuaker, J.H.S. & Gawthorpe, R.L. 1993: Mudstone lithofacies in the Kimmeridge Clay Formation, Wessex Basin, southern England; implications for the origin and controls of the distribution of mudstones. *Journal of Sedimentary Research 63*, 1129–1143. https://doi.org/10.1306/D4267CC1-2B26-11D7-8648000102C1865D

MacQuaker, J.H.S., Bentley, S.J. & Bohacs, K.M. 2010: Wave-enhanced sediment-gravity flows and mud dispersal across continental shelves: Reappraising sediment transport processes operating in ancient mudstone successions. *Geology 38*, 947–950. https://doi.org/10.1130/G31093.1

Martin, K.D. 2004: A re-evaluation of the relationship between trace fossils and dysoxia. *Geological Society of London 228*, 141–156. https://doi.org/10.1144/GSL.SP.2004.228.01.08

Maxwell, E.E. & Kear, B.P. 2013: Triassic ichthyopterygian assemblages of the Svalbard archipelago: a reassessment of taxonomy and distribution. *Journal of the Geological Society of Sweden 135*, 85–94. https://doi.org/10.1080/11035897.2012.759145

McRoberts, C.A. 2000: A primitive *Halobia* (Bivalvia : Halobioidea) from the Triassic of northeast British Columbia. *Journal of Paleontology 74,* 599–603.

https://doi.org/10.1666/0022-3360(2000)074<0599:APHBHF>2.0.CO;2
McRoberts, C.A. 2010: Biochronology of Triassic bivalves. *Geological Society, London, Special Publications 334*, 201–219. https://doi.org/10.1144/SP334.9

McRoberts, C.A. 2011: Late Triassic Bivalvia (chiefly Halobiidae and Monotidae) from the Pardonet Formation, Williston Lake Area, Northeastern British Columbia, Canada. *Journal of Paleontology 85,* 613–664. https://doi.org/10.1666/10-051.1

McRoberts, C.A., Blodgett, R.B. & Bird, K.J. 2021: Middle and Upper Triassic Bivalve Biostratigraphy of the Shublik Formation from the Tenneco Phoenix# 1 Well, Offshore Central North Slope, Arctic Alaska. *New Mexico Museum of Natural History and Science Bulletin 82,* 259–274.

Meyers, P.A. 1994: Preservation of elemental and isotopic source identification of sedimentary organic matter. *Chemical Geology 114*, 289–302. https://doi.org/10.1016/0009-2541(94)90059-0

Morford, J.L., Russell, A.D. & Emerson, S. 2001: Trace metal evidence for changes in the redox environment associated with the transition from terrigenous clay to diatomaceous sediment, Saanich Inlet, BC. *Marine Geology 174*, 355–369. https://doi.org/10.1016/S0025-3227(00)00160-2

Mørk, A., Knarud, R. & Worsley, D. 1982: Depositional and diagenetic environments of the Triassic and Lower Jurassic succession of Svalbard. *In* Embry, A.F. & Balkwill, H.R. (eds.): *Arctic Geology and Geophysics 8*, Canadian Society of Petroleum Geologists Memoir, 371–398.

Mørk, A. & Bjorøy, M. 1984: Mesozoic source rocks on Svalbard. *In* Spencer, A.M. (ed.): *Petroleum Geology of the North European Margin*, Springer Netherlands, Dordrecht, 371–382.
https://doi.org/10.1007/978-94-009-5626-1

Mørk, A., Vigran, J., Korchinskaya, M., Pchelina, T., Fefilova, L., Vavilov, M. & Weitschat, W. 1993: Triassic rocks in Svalbard, the Arctic Soviet islands and the Barents Shelf: bearing on their correlations. *In* Vorren, T.O., Bergsager, E., Dahl-Stamnes, Ø.A., Holter, E., Johansen, B., Lie, E. & Lund, T.B. (eds.): *Arctic Geology and Petroleum Potential, Norwegian Petroleum Society Special Publication 2*, Elsevier, Amsterdam, 457–479. https://doi.org/10.1016/B978-0-444-88943-0.50033-2

Mørk, A., Elvebakk, G., Forsberg, A.W., Hounslow, M.W., Nakrem, H.A., Vigran, J.O. & Weitschat, W. 1999: The type section of the Vikinghøgda Formation: a new Lower Triassic unit in central and eastern Svalbard. *Polar Research 18*, 51–82. https://doi.org/10.1111/j.1751-8369.1999.tb00277.x

Mørk, A. & Bromley, R.G. 2008: Ichnology of a marine regressive systems tract: the Middle Triassic of Svalbard. *Polar Research 27,* 339–359. https://doi.org/10.1111/j.1751-8369.2008.00077.x

Nakrem, H.A., Orchard, M.J., Weitschat, W., Hounslow, M.W., Beatty, T.W. & Mørk, A. 2008: Triassic conodonts from Svalbard and their Boreal correlations. *Polar Research 27*, 523–539.
https://doi.org/10.1111/j.1751-8369.2008.00076.x

Nathorst, A.G. 1910: Beiträge zur Geologie der Bären-Insel, Spitzbergens und des König-Karl-Landes: *Bulletin of the Geological Institution of the University of Upsala 10*, Almquist & Wiksell Boktryckeri, Uppsala, 261–415.

Noe-Nygaard, N., Surlyk, F. & Piasecki, S. 1987: Bivalve Mass Mortality Caused by Toxic Dinoflagellate Blooms in a Berriasian-Valanginian Lagoon, Bornholm, Denmark. PALAIOS 2, 263–273. https://doi.org/10.2307/3514676

Oschmann, W. 1991: Distribution, dynamics and palaeoecology of Kimmeridgian (Upper Jurassic) shelf anoxia in western Europe. *Geological Society, London, Special Publications 58*, 381–395. https://doi.org/10.1144/GSL.SP.1991.058.01.24

Pchelina, T. 1977: Permian and Triassic deposits of Edgeøya (Svalbard): Stratigraphy and Palaeontology of the Precambrian and Paleozoic of Northern Siberia. *A Collection of Scientific Papers, NIIGA, Leningrad, 59–71.*

Pietsch, C. & Bottjer, D.J. 2014: The importance of oxygen for the disparate recovery patterns of the benthic macrofauna in the Early Triassic. *Earth-Science Reviews 137,* 65–84. https://doi.org/10.1016/j.earscirev.2013.12.002

Posenato, R., Bassi, D. & Avanzini, M. 2013: Bivalve pavements from shallow-water black-shales in the Early Jurassic of northern Italy: A record of salinity- and oxygen-depleted environmental dynamics. *Palaeogeography, Palaeoclimatology, Palaeoecology 369*, 262–271. https://doi.org/10.1016/j.palaeo.2012.10.032

Rhoads, D.C. & Morse, J.W. 1971: Evolutionary and ecologic significance of oxygen-deficient marine basins. *Lethaia 4*, 413–428. https://doi.org/10.1111/j.1502-3931.1971.tb01864.x

Riis, F., Lundschien, B.A., Høy, T., Mørk, A. & Mørk, M.B.E. 2008: Evolution of the Triassic shelf in the northern Barents Sea region. *Polar Research 27*, 318–338. https://doi.org/10.1111/j.1751-8369.2008.00086.x

Roberts, A., Engelschiøn, V.S. & Hurum, J. 2022: First three-dimensional skull of the Middle Triassic ichthyosaur *Phalarodon fraasi* (Mixosauridae) from Svalbard, Norway. *Acta Palaeontologica Polonica 67*, 51–62. https://doi.org/10.4202/app.00915.2021

Rueden, C.T., Schindelin, J., Hiner, M.C., DeZonia, B.E., Walter, A.E., Arena, E.T. & Eliceiri, K.W. 2017: ImageJ2: ImageJ for the next generation of scientific image data. *BMC Bioinformatics 18*, 529–529. https://doi.org/10.1186/s12859-017-1934-z

Sampei, Y. & Matsumoto, E. 2001: C/N ratios in a sediment core from Nakaumi Lagoon, southwest Japan. Usefulness as an organic source indicator. *GEOCHEMICAL JOURNAL 35,* 189–205. https://doi.org/10.2343/geochemj.35.189

Savrda, C.E. & Bottjer, D.J. 1989: Trace-fossil model for reconstructing oxygenation histories of ancient marine bottom waters: Application to Upper Cretaceous Niobrara Formation, Colorado. *Palaeogeography, Palaeoclimatology, Palaeoecology 74*, 49–74. https://doi.org/10.1016/0031-0182(89)90019-9

Schatz, W. 2001: Taxonomic significance of biometric characters and the consequences for classification and biostratigraphy, exemplified through moussoneliform daonellas (*Daonella*, Bivalvia; Triassic). *Paläontologische Zeitschrift 75*, 51–70. https://doi.org/10.1007/BF03022598

Schatz, W. 2004: Revision of the subgenus *Daonella* (*Arzelella*) (Halobiidae; Middle Triassic). *Journal of Paleontology 78*, 300–316. https://doi.org/10.1666/0022-3360(2004)078<0300:ROTSDA>2.0.CO;2

Schatz, W. 2005: Palaeoecology of the Triassic black shale bivalve Daonella—new insights into an old controversy. *Palaeogeography, Palaeoclimatology, Palaeoecology 216,* 189–201. https://doi.org/10.1016/j.palaeo.2004.11.002

Schindelin, J., Arganda-Carreras, I., Frise, E., Kaynig, V., Longair, M., Pietzsch, T., Preibisch, S., Rueden, C., Saalfeld, S., Schmid, B., Tinevez, J.-Y., White, D.J., Hartenstein, V., Eliceiri, K., Tomancak, P. & Cardona, A. 2012: Fiji: an open-source platform for biological-image analysis. *Nature Methods 9*, 676–682. https://doi.org/10.1038/nmeth.2019

Sellwood, B. 1971: A *Thalassinoides* burrow containing the crustacean *Glyphaea udressieri* (Meyer) from the Bathonian of Oxfordshire. *Palaeontology 14*, 589–591.

Simões, M.G. & Kowalewski, M. 1998: Shell beds as paleoecological puzzles: A case study from the Upper Permian of the Paraná Basin, Brazil. *Facies 38*, 175–195. https://doi.org/10.1007/BF02537364

Song, H., Wignall, P.B., Chu, D., Tong, J., Sun, Y., Song, H., He, W. & Tian, L. 2014: Anoxia/high temperature double whammy during the Permian-Triassic marine crisis and its aftermath. *Scientific Reports 4*, 4132–4132. https://doi.org/10.1038/srep04132

Song, H., Wignall, P.B. & Dunhill, A.M. 2018: Decoupled taxonomic and ecological recoveries from the Permo-Triassic extinction. *Science Advances 4,* eaat5091. https://doi.org/10.1126/sciadv.aat5091

Tozer, E. 1961: Triassic stratigraphy and faunas, Queen Elizabeth Islands, Arctic Archipelago. *Geological Survey of Canada 316*, 65–12. https://doi.org/10.4095/100543

Tozer, E. & Parker, J. 1968: Notes on the Triassic biostratigraphy of Svalbard. *Geological Magazine 105*, 526–542. https://doi.org/10.1017/S0016756800055886

Vigran, J.O., Mørk, A., Forsberg, A.W., Weiss, H.M. & Weitschat, W. 2008: Tasmanites algae-contributors to the Middle Triassic hydrocarbon source rocks of Svalbard and the Barents Shelf. *Polar Research 27*, 360–371. https://doi.org/10.1111/j.1751-8369.2008.00084.x

Vigran, J.O., Mangerud, G., Mørk, A., Worsley, D. & Hochuli, P.A. 2014: Palynology and geology of the Triassic succession of Svalbard and the Barents Sea. *Geological Survey of Norway Special Publication 14*, 1–269. https://doi.org/10.5167/uzh-99116

von Mojsvár, E.M. 1886: Arktische Triasfaunen. Beiträge zur paläontologischen Charakteristik der Arktisch-Pacifischen Triasprovinz. *Mémoires de l'Académie Impériale des Sciences de St. Petersburg Séries 7,* 1–59.

Weitschat, W. & Lehmann, U. 1983: Stratigraphy and ammonoids from the Middle Triassic Botneheia Formation (Daonella Shales) of Spitsbergen. *Mitteilungen aus dem Geologisch-Paläontologischen Institut der Universität Hamburg* 54, 27–54.

Wesenlund, F., Grundvåg, S.-A., Engelschiøn, V.S., Thießen, O. & Pedersen, J.H. 2021: Linking facies variations, organic carbon richness and bulk bitumen content – A case study of the organic-rich Middle Triassic shales from eastern Svalbard. *Marine and Petroleum Geology 132,* 105168–105195. https://doi.org/10.1016/j.marpetgeo.2021.105168

Wesenlund, F., Grundvåg, S.A., Engelschiøn, V.S., Thießen, O. & Pedersen, J.H. 2022: Multi-elemental chemostratigraphy of Triassic mudstones in eastern Svalbard: Implications for source rock formation in front of the World's largest delta plain. *The Depositional Record 8*, 718–753. https://doi.org/10.1002/dep2.182

Wignall, P.B. 1993: Distinguishing between oxygen and substrate control in fossil benthic assemblages. *Journal of the Geological Society 150,* 193–196. https://doi.org/10.1144/gsjgs.150.1.0193

Wignall, P.B. & Twitchett, R.J. 1996: Oceanic Anoxia and the End Permian Mass Extinction. *Science 272*, 1155–1158. https://doi.org/10.1126/science.272.5265.1155

Wignall, P.B., Morante, R. & Newton, R. 1998: The Permo-Triassic transition in Spitsbergen: δ13Corg chemostratigraphy, Fe and S geochemistry, facies, fauna and trace fossils. *Geological Magazine 135*, 47–62. https://doi.org/10.1017/S0016756897008121

Wignall, P.B., Bond, D.P.G., Grasby, S.E., Pruss, S.B. & Peakall, J. 2020: Controls on the formation of microbially induced sedimentary structures and biotic recovery in the Lower Triassic of Arctic Canada. *GSA Bulletin 132*, 918–930. https://doi.org/10.1130/B35229.1

Wiman, C. 1916: Notes on the marine Triassic reptile fauna of Spitzbergen. *Bulletin of the Department of Geology 10, University of California publications, Berkeley,* 63–73.

Yanin, B. & Baraboshkin, E.Y. 2013: *Thalassinoides* burrows (Decapoda dwelling structures) in Lower Cretaceous sections of southwestern and central Crimea. *Stratigraphy and Geological correlation 21*, 280–290. https://doi.org/10.1134/S086959381303009X

Zhang, F., Romaniello, S.J., Algeo, T.J., Lau, K.V., Clapham, M.E., Richoz, S., Herrmann, A.D., Smith, H., Horacek, M. & Anbar, A.D. 2018: Multiple episodes of extensive marine anoxia linked to global warming and continental weathering following the latest Permian mass extinction. *Science Advances 4,* e1602921. https://doi.org/10.1126/sciadv.1602921

Økland, I.H., Delsett, L.L., Roberts, A.J. & Hurum, J.H. 2018: A *Phalarodon fraasi* (Ichthyosauria: Mixosauridae) from the Middle Triassic of Svalbard. *Norwegian Journal of Geology 98*, 267–288. https://doi.org/10.17850/njg98-2-06